Anal. Chem. **2008,** *80,* 1425−1436

Surface-Induced Dissociation of Peptides and Protein Complexes in a Quadrupole/Time-of-Flight Mass Spectrometer

Asiri S. Galhena, Shai Dagan,† Christopher M. Jones, Richard L. Beardsley, and Vicki H. Wysocki*

Department of Chemistry, University of Arizona, 1306E University Boulevard, Tucson, Arizona 85721

A novel in-line surface-induced dissociation (SID) device was designed and implemented in a commercial QTOF instrument (Waters/Micromass QTOF II). This new setup allows efficient SID for a broad range of molecules. It also allows direct comparison with conventional collision-induced dissociation (CID) on the same instrument, taking advantage of the characteristics of QTOF instrumentation, including extended mass range, improved sensitivity, and better resolution compared with quadrupole analyzers and ion traps. Various peptides and a noncovalent protein complex have been electrosprayed and analyzed with the new SID setup. Here we present SID of leucine enkephalin, fibrinopeptide A, melittin, insulin chain-B, and a noncovalent protein complex from wheat, heat shock protein 16.9. The SID spectra were also compared to CID spectra. With the SID setup installed, ion transmission proved to be efficient. SID fragmentation patterns of peptides are, in general, similar to CID, with differences in the relative intensities of some peaks such as immonium ions, backbone cleavage b- versus y-type ions, and y- versus y-NH_3 ions, suggesting enhanced accessibility to high-energy/secondary fragmentation channels with SID. Furthermore, these results demonstrate that the in-line SID setup is a valid substitute for CID, with potential advantages for activation of singly/multiply charged peptides and larger species such as noncovalent protein complexes.

Tandem mass spectrometry is a well-established analytical technique for the characterization and identification of molecular structures. This technique involves activation of precursor ions followed by mass analysis of the fragment ion products.[1] The nature of ion fragmentation depends on the method of ion activation. The most common activation method, collision-induced dissociation (CID)[2,3] or collisionally activated dissociation, involves precursor ion excitation via multiple collisions with an inert gas. An ion of given translational energy undergoes a series of inelastic collisions with the neutral gas, and a fraction of its translational energy is converted into internal energy, leading to subsequent fragmentation.[2] The efficiency of CID is dependent on the relative masses of the target gas and the colliding ion.[1] The lower the mass of the target gas, the lower the internal energy in the center of mass reference frame. Traditionally, in order to limit scattering, CID targets have been low-mass inert gases such as He or Ar; therefore, even with multiple collisions, the total energy conversion is limited. This property sometimes limits the utility of CID when dealing with large, complex biological molecules such as intact proteins or noncovalent complexes, which can require high activation energy to induce dissociation.

Surface-induced dissociation (SID) is an alternative collisional activation method, first introduced by Cooks and co-workers.[4,5] This technique has been used by several research groups to analyze small molecules,[6] peptides,[7−14] and even proteins.[9,15,16] Cooks recently published an extensive review that covers the fundamentals of SID and the current level of understanding of the SID process.[17] Ion activation in SID is analogous to CID, except that a target surface is used as a collision target instead of inert gas. SID more closely approximates a single collision process compared to multiple collisions in CID. Among the various types of surfaces extensively explored for SID,[18−26] fluorinated self-

* To whom correspondence should be addressed. Phone: 520-621-2628. Fax: 520-621-8407. E-mail: vwysocki@email.arizona.edu.

† Present address: Israel Institute for Biological Research (IIBR), P.O. Box 19, Ness Ziona, 74100, Israel.

(1) Sleno, L.; Volmer, D. A. *J. Mass Spectrom.* **2004**, *39*, 1091−1112.
(2) Mcluckey, S. A. *J. Am. Soc. Mass Spectrom.* **1992**, *3*, 599−614.
(3) Shukla, A. K.; Futrell, J. H. *J. Mass Spectrom.* **2000**, *35*, 1069−1090.
(4) Cooks, R. G.; Terwilliger, D. T.; Ast, T.; Beynon, J. H.; Keough, T. *J. Am. Chem. Soc.* **1975**, *97*, 1583−1585.
(5) Cooks, R. G.; Ast, T.; Beynon, J. H. *Int. J. Mass Spectrom. Ion Processes* **1975**, *16*, 348−352.
(6) Vekey, K.; Somogyi, A.; Wysocki, V. H. *J. Mass Spectrom.* **1995**, *30*, 212−217.
(7) Tsaprailis, G.; Nair, H.; Somogyi, A.; Wysocki, V. H.; Zhong, W. Q.; Futrell, J. H.; Summerfield, S. G.; Gaskell, S. J. *J. Am. Chem. Soc.* **1999**, *121*, 5142−5154.
(8) Durkin, D. A.; Schey, K. L. *Int. J. Mass Spectrom.* **1998**, *174*, 63−71.
(9) Dongre, A. R.; Somogyi, A.; Wysocki, V. H. *J. Mass Spectrom.* **1996**, *31*, 339−350.
(10) Nair, H.; Wysocki, V. H. *Int. J. Mass Spectrom.* **1998**, *174*, 95−100.
(11) Laskin, J.; Denisov, E.; Futrell, J. *J. Am. Chem. Soc.* **2000**, *122*, 9703−9714.
(12) Jackson, A. T.; Despeyroux, D.; Jennings, K. R. *Int. J. Mass Spectrom. Ion Processes* **1995**, *141*, 91−99.
(13) Mccormack, A. L.; Somogyi, A.; Dongre, A. R.; Wysocki, V. H. *Anal. Chem.* **1993**, *65*, 2859−2872.
(14) Sun, W. J.; May, J. C.; Russell, D. H. *Int. J. Mass Spectrom.* **2007**, *259*, 79−86.
(15) Chorush, R. A.; Little, D. P.; Beu, S. C.; Wood, T. D.; Mclafferty, F. W. *Anal. Chem.* **1995**, *67*, 1042−1046.
(16) Stone, E.; Gillig, K. J.; Ruotolo, B.; Fuhrer, K.; Gonin, M.; Schultz, A.; Russell, D. H. *Anal. Chem.* **2001**, *73*, 2233−2238.
(17) Grill, V.; Shen, J.; Evans, C.; Cooks, R. G. *Rev. Sci. Instrum.* **2001**, *72*, 3149−3179.

10.1021/ac701782q CCC: $40.75
Published on Web 02/02/2008

assembled monolayer (FSAM) surfaces composed of well-ordered fluorinated alkanethiolates on gold are often chosen, because they provide minimal neutralization, efficient projectile internal energy deposition, and long-term stability. These properties make FSAM surfaces attractive for SID and provide fragmentation efficiencies comparable to or better than CID, depending on experimental conditions, where fragmentation efficiency is defined as the ratio of ∑(fragment ion intensity)/∑(total ion intensity (precursor + fragments).

It has been demonstrated that, with SID, a significant amount of precursor ion translational energy is converted into internal energy causing fragmentation.[27−31] This is explained by the higher effective mass of the surface compared to masses of typical CID gases, leading to higher energies in the center of mass frame of reference. This higher internal energy deposition offers the possibility of dissociating very large molecules or complexes that are difficult to activate by CID. In addition, SID may offer the potential advantage of improved ion collection efficiency compared to CID, where the multiple collision conditions used in CID may cause scattering of the ion beam.[32] When comparing internal energy distributions, SID has been shown to offer a narrow controllable internal energy distribution relative to single collision kiloelectronvolt CID.[28] With respect to multiple collision electronvolt CID of small peptides, Laskin and co-workers have demonstrated that the width of the energy distribution is similar for SID and CID in an FTICR instrument.[11] The fine control over the internal energy deposition has led to a better fundamental understanding of ion dissociation mechanisms.[33]

To date, SID has been carried out in several different types of mass spectrometers.[16,34−37] Wysocki et al.[38] have reported an orthogonally configured SID setup for small organic compounds and peptides in a quadrupole-surface-quadrupole instrument. This is a simplification of an earlier design by Bier et al.[39] Although this design is very successful, incorporation of an orthogonal surface assembly into most commercially available mass spectrometers would require major instrument modifications from their linear configurations. Although significant progress has been made in the development of SID instrumentation and the understanding of SID collision processes, the application of SID as a routine and effective activation method in commercial mass spectrometers has yet to be realized.

Our goal was to incorporate a simple SID device into a quadrupole/time-of-flight mass spectrometer (QTOF) with minimal instrument modification so as not to disturb the original instrument performance. We have therefore designed an in-line SID device that can be incorporated easily into the original configuration of this commercial instrument. While the incorporation of a limited number of in-line SID devices in different MS instruments has already been reported,[35,38,40−43] no in-line SID devices have been demonstrated in an ESI-QTOF instrument. Implementation of SID in such an instrument has significant advantages in resolution and m/z range over previously reported SID instruments. Furthermore, the QTOF mass spectrometer is a robust instrument equipped with unique capabilities such as high sensitivity, high mass resolution, and high mass accuracy, in both the MS and MS/MS modes.[44] The most recent installation of an in-line SID device in a TOF instrument was reported by the Russell group in a MALDI-ion mobility-orthogonal TOF instrument.[16] This particular instrument uses a hydrocarbon-coated gold grid (90% transmission) as the collision target. However, an improved version of the same instrument, by coupling SID in an orthogonal configuration, was later reported by the same group.[14] One of the advantages of this orthogonal design is that it could perform surface-normal SID that would provide optimal energy conversion by SID. Gaskell and co-workers also reported SID installation in a modified triple-quadrupole mass spectrometer.[37] Even though this instrument required an orthogonally coupled quadrupole mass analyzer at the back end of the triple quadrupole, the capability of performing CID and SID in the same instrument was a distinct advantage.

We report here the modification of a commercially available QTOF mass spectrometer to accommodate SID as an additional ion activation method to complement CID. The design allows comparison between the two ion activation methods. In addition, combination of these two activation methods allows more extensive fragmentation and collisional focusing phenomena to be explored. The performance of this in-line SID device is demonstrated here by analyzing several peptides and a noncovalent protein complex.

(18) Tillman, N.; Ulman, A.; Penner, T. L. *Langmuir* **1989**, *5*, 101−111.
(19) Nuzzo, R. G.; Allara, D. L. *J. Am. Chem. Soc.* **1983**, *105*, 4481−4483.
(20) Porter, M. D.; Bright, T. B.; Allara, D. L.; Chidsey, C. E. D. *J. Am. Chem. Soc.* **1987**, *109*, 3559−3568.
(21) Allara, D. L.; Nuzzo, R. G. *Langmuir* **1985**, *1*, 52−66.
(22) Allara, D. L.; Nuzzo, R. G. *Langmuir* **1985**, *1*, 45−52.
(23) Strong, L.; Whitesides, G. M. *Langmuir* **1988**, *4*, 546−558.
(24) Bain, C. D.; Troughton, E. B.; Tao, Y. T.; Evall, J.; Whitesides, G. M.; Nuzzo, R. G. *J. Am. Chem. Soc.* **1989**, *111*, 321−335.
(25) Nuzzo, R. G.; Dubois, L. H.; Allara, D. L. *J. Am. Chem. Soc.* **1990**, *112*, 558−569.
(26) Bryant, M. A.; Pemberton, J. E. *J. Am. Chem. Soc.* **1991**, *113*, 3629−3637.
(27) Cooks, R. G.; Ast, T.; Mabud, A. *Int. J. Mass Spectrom. Ion Processes* **1990**, *100*, 209−265.
(28) Dekrey, M. J.; Kenttamaa, H. I.; Wysocki, V. H.; Cooks, R. G. *Org. Mass Spectrom.* **1986**, *21*, 193−195.
(29) Morris, M. R.; Riederer, D. E.; Winger, B. E.; Cooks, R. G.; Ast, T.; Chidsey, C. E. D. *Int. J. Mass Spectrom. Ion Processes* **1992**, *122*, 181−217.
(30) Miller, S. A.; Riederer, D. E.; Cooks, R. G.; Cho, W. R.; Lee, H. W.; Kang, H. *J. Phys. Chem.* **1994**, *98*, 245−251.
(31) Pradeep, T.; Miller, S. A.; Cooks, R. G. *J. Am. Soc. Mass Spectrom.* **1993**, *4*, 769−773.
(32) Dawson, P. H.; Douglas, D. J. *Int. J. Mass Spectrom. Ion Processes* **1983**, *47*, 121−124.
(33) Dongre, A. R.; Jones, J. L.; Somogyi, A.; Wysocki, V. H. *Abstr. Pap. Am. Chem. S* **1994**, *208*, 50-Anyl.
(34) Williams, E. R.; Henry, K. D.; Mclafferty, F. W.; Shabanowitz, J.; Hunt, D. F. *J. Am. Soc. Mass Spectrom.* **1990**, *1*, 413−416.
(35) Ijames, C. F.; Wilkins, C. L. *Anal. Chem.* **1990**, *62*, 1295−1299.
(36) Lammert, S. A.; Cooks, R. G. *J. Am. Soc. Mass Spectrom.* **1991**, *2*, 487−491.
(37) Mohammed, S.; Chalmers, M. J.; Gielbert, J.; Ferro, M.; Gora, L.; Smith, D. C.; Gaskell, S. J. *J. Mass Spectrom.* **2001**, *36*, 1260−1268.
(38) Wysocki, V. H.; Ding, J. M.; Jones, J. L.; Callahan, J. H.; King, F. L. *J. Am. Soc. Mass Spectrom.* **1992**, *3*, 27−32.
(39) Bier, M. E.; Amy, J. W.; Cooks, R. G.; Syka, J. E. P.; Ceja, P.; Stafford, G. *Int. J. Mass Spectrom. Ion Processes* **1987**, *77*, 31−47.
(40) Bier, M. E.; Schwartz, J. C.; Schey, K. L.; Cooks, R. G. *Int. J. Mass Spectrom. Ion Processes* **1990**, *103*, 1−19.
(41) Li, G.; Duhr, A.; Wollnik, H. *J. Am. Soc. Mass Spectrom.* **1992**, *3*, 487−492.
(42) Wright, A. D.; Despeyroux, D.; Jennings, K. R.; Evans, S.; Riddoch, A. *Org. Mass Spectrom.* **1992**, *27*, 525−526.
(43) Despeyroux, D.; Wright, A. D.; Jennings, K. R.; Evans, S.; Riddoch, A. *Int. J. Mass Spectrom. Ion Processes* **1992**, *122*, 133−141.
(44) Chernushevich, I. V.; Loboda, A. V.; Thomson, B. A. *J. Mass Spectrom.* **2001**, *36*, 849−865.

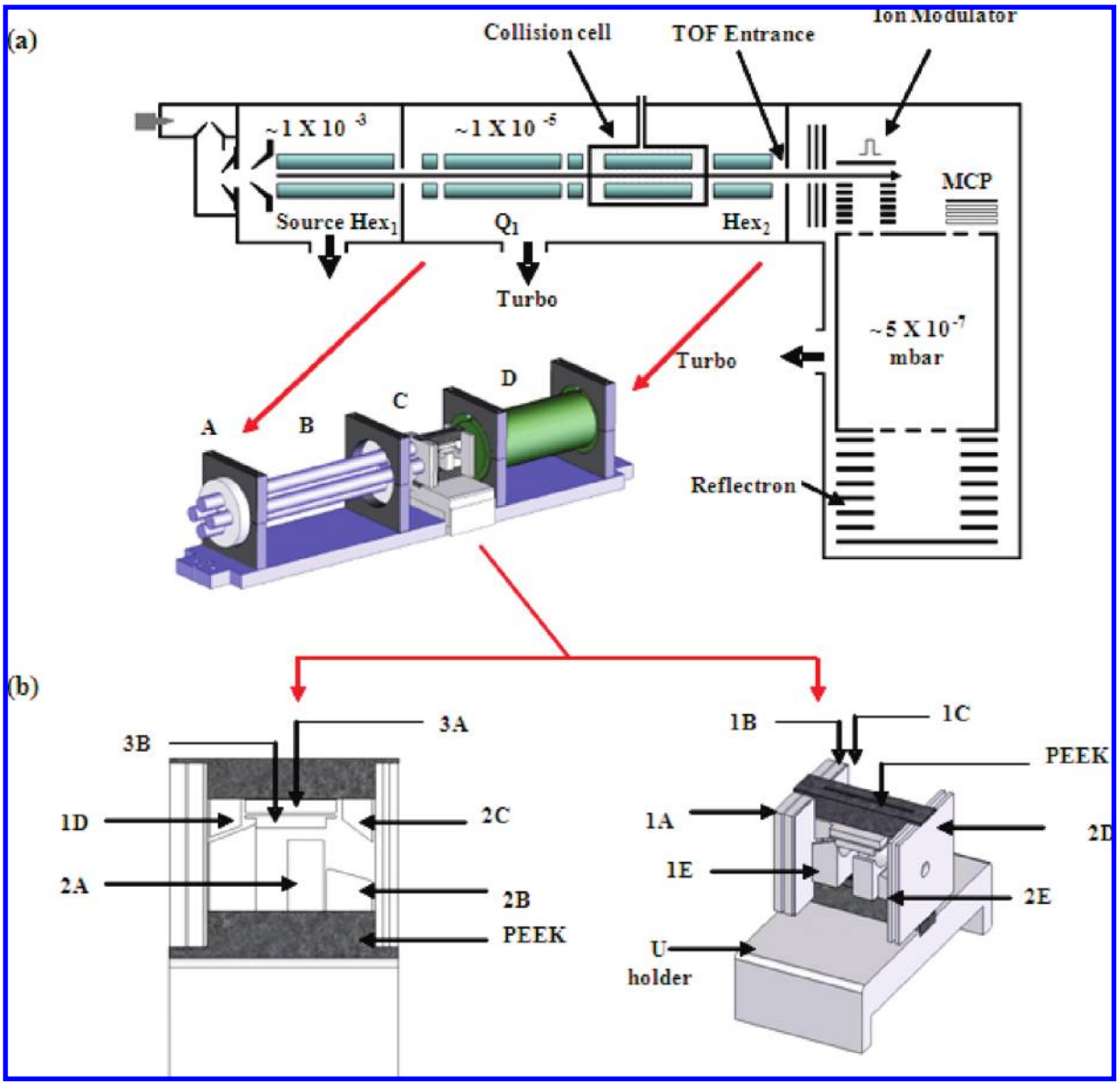

Figure 1. (a) Schematic of the QTOF instrument and a blow-up of the new in-line SID set up installation region. The hexapole ion guide (Hex_2) was removed, the collision cell was moved (right) toward the TOF entrance, and the new SID setup was installed between the quadrupole analyzer Q_1 and the collision cell. (b) Schematics of the side view of the setup, mounted on a base (left) and a 3D view of the setup (right). The incoming beam is focused by entrance lenses 1A, 1B, and 1C and then deflected up by the bottom U deflector (1E) and top deflector (1D). The surface is mounted on the surface holder 3A with a square lens attached to it (3B). The product ion beam is deflected back by the bottom U (2B) and top (2C) deflectors and focused by exit lenses 2D and 2E.

EXPERIMENTAL SECTION

Modification of a Commercial Quadrupole/Time-of-Flight Mass Spectrometer for SID Operation. Instrumentation. A quadrupole/time-of-flight mass spectrometer (QTOF II, Micromass/Waters, Manchester, UK) was modified to accommodate the in-line SID setup by removing the ion-transfer hexapole (Hex_2 - Figure 1a) and repositioning the collision cell toward the time-of-flight chamber. The repositioning of the collision cell required two new threaded holes in the bottom rail. The SID setup was installed between the quadrupole (Q1) and the collision cell (Figure 1a). The top aluminum cover of the quadrupole chamber was machined to hold 14 mountable BNC female connectors (Part No. 31-102, Amphenol RF, Danbury, CT). No additional machining or modification of any of the remaining hardware was required to install the SID setup.

The SID setup (Figure 1b) consists of three main functional regions: a precursor ion focusing region, a surface region, and a fragment ion extraction region. The precursor ion focusing region (labeled as 1A−E in Figure 1b) guides and focuses the ion beam onto the collision surface. This region consists of three stainless steel square lenses, followed by a "U"-shaped precursor ion deflector (1E in Figure 1b.) and a flat precursor ion deflector (item 1D in Figure 1b). The first two square lenses have a thickness of 3 mm and the final square lens is 0.80 mm. All three squares are 36 mm × 36 mm with a 5-mm-inner diameter orifice (center bored openings). The two deflectors at the entrance (top 1D and bottom 1E) serve to deflect the precursor ions onto the surface. The U-shaped deflector has a width of 14 mm, height of 16.5 mm, and thickness of 9 mm. It has a 6-mm radius from center and was

machined with an ~20° angle up-slope from front to back. The top precursor ion deflector has a width of 12 mm, height of 7.5 mm, and thickness of 6 mm. The lower surface of the top deflector was machined to have an ~20° slope like that of the precursor ion U deflector. Both the top and bottom precursor ion deflectors were mounted ~1 mm from the third entrance square lens (1C in Figure 1b).

The surface assembly region (3A,B in Figure 1b) consists of an 18 mm × 18 mm × 2.5 mm stainless steel mounting holder (3A in Figure 1b) positioned in parallel with the incoming ion beam (8 mm above the center of the ion beam to allow ~45° collision angle), followed by an ion extraction hollow square lens that is attached (3B in Figure 1b) to the surface holder.

The fragment ion extraction region focuses the ions leaving the collision target. This region consists of three deflectors followed by two square lenses (2A−E in Figure 1b). The fragment U deflector has the same morphology as the precursor ion U deflector, having a width of 18 mm, height of 14 mm, and thickness of 7 mm. The curvature of the U has an 8-mm radius compared to 6 mm in the precursor U deflector and was installed ~15 mm beyond the third square entrance lens. Immediately after the fragment U deflector is a flat bottom fragment deflector with a thickness of 9 mm, which is installed ~22 mm from the third square entrance lens. The top edge of the deflector is machined to have a flat slope, about ~20° downward from front to back. The top fragment deflector with a width of 12 mm, a height of 8.5 mm, and thickness of 6 mm, was installed ~27 mm beyond the final square entrance lens and was machined to have a ~20° slope downward from front to back. The two fragment ion exit square lenses were machined to be 36 mm × 36 mm × 1.5 mm with a 5-mm-inner diameter circular center bored opening.

The ion deflectors, square lenses, and surface holders are supported by two top and bottom polyetheretherketone (PEEK) (McMaster-Carr) blocks. The bottom PEEK block is stationary on an aluminum base and mounted between the quadrupole and the collision cell (Figure 1a,b). The position of the base was set to have a minimum of 3-mm spacing from the quadrupole post filter and the collision cell. The electrical connections to each of the elements of the SID setup were wired with coaxial cables (Part No. MIL-C-17G 50 Ohm coaxial cable, Belden CDT Electronics, Richmond, IN) and screw tightened. The free ends of the cables were soldered into BNC connectors on the lid of the quadrupole chamber.

Q-SID/CID-TOF Operation. As mentioned before, the SID setup can be operated in two modes: one that allows surface collisions and another that transmits ions for MS or CID operation. For both modes, the peptide samples were introduced by direct infusion at a flow rate of 5 μL/min to the conventional electrospray probe. The ESI capillary voltage was operated in a range of 2.6−3.6 keV, and the sample cone was set to operate at 20 − 60 V. For the experiments on noncovalent protein complexes, samples were introduced by a home-built nano-ESI spray source, with the capillary operated in a range of ~1.5−2 keV and the cone voltage at ~120 V. For both CID and SID experiments, the quadrupole analyzer served as a precursor ion selector and the TOF served as a high-resolution product ion analyzer. Except for the SID/CID components, the default instrument settings were employed.

In CID mode, the experiments were performed using argon as the target gas. The collision pressure is reported as the pressure at the quadrupole mass analyzer chamber (the actual pressure in the collision cell is different from the quadrupole chamber pressure); however, due to the lack of a pressure gauge connected to the collision cell, the pressure in the quadrupole chamber region is reported as collision pressure. The typical quadrupole chamber gas pressure used for CID operation is ~3×10^{-5} mbar). The CID collision voltage was controlled by adjusting the dc offset of the source hexapole (Figure 1a, Hex_1) between 0 and 200 V relative to the collision cell (grounded). The appropriate voltage setting of the SID device for noncollision fly-through CID operation was achieved by increasing the surface voltage while reducing the voltages of the two U deflectors until the total ion count (TIC) at the TOF detector (MCP) was optimized (typical voltages of the SID device in the fly-through mode are shown in Figure 2a).

The SID mode was operated in a fashion similar to CID, where the collision voltage is varied between 0 and 190 V by setting the dc offset (10−200 V) of the source hexapole (Hex_1) with respect to the surface voltage (~10−20 V). The actual collision voltage was calculated by subtracting the difference between these two voltages. The voltage settings for the SID device in the SID operation mode (Figure 2b) were achieved by increasing the precursor U deflector voltage to direct ions to the surface and fine-tuning the other SID elements to extract fragment ions and optimize the TIC at the TOF detector (MCP). Note: Throughout this paper, all the collision voltages are presented as charge corrected collision energies; i.e., 20 V collision of a doubly protonated projectile is represented as 40 eV collision energy.

Materials and Samples. SAM Surfaces. Glass surfaces (18 mm × 12 mm) coated with a 10-Å layer of titanium followed by a 1000-Å layer of gold (Evaporated Metal films Corp., Ithaca, NY) were used as substrates for the SID collision targets. The Au-coated glass slide was first UV cleaned for 15 min, rinsed with ethanol, and immersed in a 1 mM ethanolic solution of 2-(perfluorodecyl)ethanethiol for 24 h. Following this step, the surface was immersed in ethanol (96% purity) and sonicated for 5 min in an ultrasonic bath. Sonication was repeated two more times with fresh ethanol solutions. Finally, the glass surfaces, coated with a fluorinated self-assembled monolayer (SAM), were air-dried and attached to the surface holder of the SID setup. The surface preparation technique is further explained elsewhere.[45,46] The 2-(perfluorodecyl)ethanethiol used for SAM surfaces was synthesized by the Chemical Synthesis Facility of the Department of Chemistry, University of Arizona.

Sample Preparation. All peptides used throughout this work were purchased from Sigma-Aldrich Chemical Co. (St. Louis, MO) and were used without any further purification. For electrospray, peptides were dissolved in $CH_3OH.H_2O$.acetic acid (50:49:1) solution to give concentrations between 20 and 100 μM.

*Ta*HSP16.9 samples were provided by Dr. Elizabeth Vierling and stored at −20 °C. Prior to nanospray MS analysis, the samples were buffer exchanged into 10 mM ammonium acetate, pH 7.0, using microcentrifuge columns (Bio-Spin, Bio-Rad). The samples were loaded into glass capillaries pulled in-house (Sutter Instru-

(45) Kane, T. E.; Somogyi, A.; Wysocki, V. H. *Org. Mass Spectrom.* **1993**, *28*, 1665−1673.
(46) Callahan, J. H.; Somogyi, A.; Wysocki, V. H. *Rapid Commun. Mass Spectrom.* **1993**, *7*, 693−699.

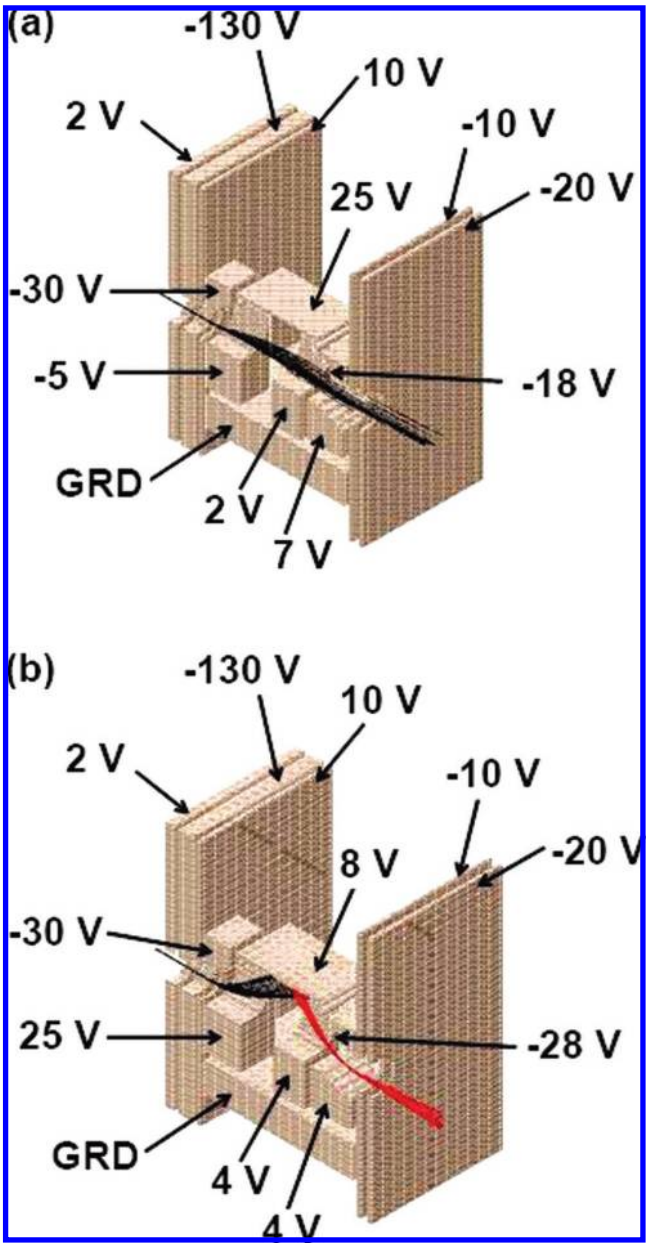

Figure 2. SIMION trajectory simulations of the SID setup. (a) Ion trajectories in the collision (SID) mode (black, precursor ion collision; red, fragment ion extraction). (b) Ion trajectories in the fly-through (MS, CID) mode, with typical operating voltages for the electrostatic elements.

ments, P-97 micropipet puller) to a final tip diameter of 1−5 μm. A platinum wire was inserted into the glass capillary, and a voltage of 1.5−2 kV was applied to electrospray the ions.

Ion Optics Simulations. The ion trajectory simulations were carried out using SIMION v. 7.0 (Idaho National Engineering and Environmental Laboratory, Idaho Falls, ID). The main goal of the simulations was to understand and optimize an in-line SID design with optimal ion transmission efficiency. Since the simulations were performed without considering any fringing fields created by surrounding electrostatic/dynamic elements, the initial simulation parameters of the precursor and fragment ion beams were chosen to have a broad variation. This takes into account the energy distributions of ions in the source and angular distribution of ions exciting the quadrupole. A beam with broad energy and angular distributions is much more challenging to guide and focus but made the SIMION simulation more realistic.

A representative SIMION simulation of the design is shown in Figure 2. The simulations were carried out in two modes: noncollision mode (fly through) for both MS and CID measurements and collision mode for SID experiments. In the noncollision fly-through mode, the simulations were performed with a packet of 20 ions similar to the ion packet defined in the precursor ion collision mode. A number of different m/z ions with different kinetic energy spreads were simulated, and results are shown here for ions of m/z 1000 (Figure 2a). The initial kinetic energy spread of the ion packet was defined to be between 5 and 15 eV. The simulation clearly indicated the ability of the SID device to transmit ions with both the low and high kinetic energies without any transmission loss.

The collision mode was subdivided into two parts, precursor ion collision and fragment ion extraction, because SIMION assumes ion neutralization upon surface collision (Figure 2b). In the precursor ion collision mode, simulation of a precursor ion of m/z 1000 colliding onto the surface is shown (Figure 2b, ion beam marked in black). The incoming precursor ion beam was defined as a packet of 20 ions. The kinetic energy of the precursor ions shown in the simulation was set to spread in a range between 50 and 60 eV. Based on previous studies reported by Collette et al.,[47] an approximate energy spread of 10 eV was used for simulations (note: simulations of different energy ranges and angular spreads were performed for both the collisional mode and for the noncollisional mode). The angular distribution of the precursor ions was set to have an elevation angle[48] spread of ±10° and azimuth angle spread of ±10° off the laboratory X axis (the optimum angular spread without any ion transmission loss was obtained at a ±10° spread). The fragment ion extraction mode was modeled as a packet of 20 ions, with a broad distribution of masses (Figure 2b, ion beam marked in red). The fragment ions departing the collision surface were defined as singly charged ions in the range of 100 to 1000 Da. The kinetic energy of the fragment ions shown in the simulation was spread between 2 and 8 eV (These are estimated kinetic energy spreads used for the purpose of SIMION modeling. However, later, experimentally measured kinetic energy spread for the fragments leaving the surface was found to be between 3 and 9 eV). The angular distribution of the fragment ions was set to have an optimum elevation angle spread of ±10° and azimuth angle of −45° with ±15° variation off the laboratory X axis without loss of any ion transmission.

RESULTS AND DISCUSSION

Implementation of SID in a Commercial QTOF Mass Spectrometer. Figure 1 shows the in-line SID setup implemented in the QTOF instrument. Our main objective was to develop a simple and robust SID design with minimal instrument modification to allow the study of fragmentation behavior of small molecules, peptides, proteins, and noncovalent complexes. In order to implement SID in a QTOF instrument, two adequate locations, the TOF region and the quadrupole region (Figure 1a), were considered. Several research groups have already performed

(47) Collette, C.; De Pauw, E. *Rapid Commun. Mass Spectrom.* **1998**, *12*, 165−170.
(48) Dahl, D. A. *Simion 3D Version 7.0 User Manual*; Bechtel Bwxt Idaho, LLC, 2000.

SID in the reflectron region of a TOF chamber.[49−52] One major limitation of such SID instruments is the loss of reflectron functionality, which results in poor TOF performance (i.e., loss of resolution). Another limitation of SID in a reflectron is the narrow observation time window for fragment ions that limits the types of product ions that may be observed.[53] The second option was to implement SID in the quadrupole/hexapole region, which would not compromise TOF performance. The limited space available in the quadrupole region restricts the SID design to be in-line rather than orthogonal if major modifications are to be avoided. The concept of in-line SID was originated by Bier et al.[40] and has been further improved by several other groups.[16,38,43,52,54,55] None of these in-line SID devices were tested for a broad range of molecules, especially not for proteins or large noncovalent protein complexes. A main consideration in our SID design was obtaining highly efficient SID/CID performance for a broad range of analytes. This was a challenge, especially for large and relatively slow moving precursor and fragment ions.

Performance of SID: CID/SID Comparison. One of the important questions addressed in this research is how the in-line SID performance compares to CID over a broad m/z range. The key issues are precursor and fragment ion transmission efficiency, energy deposition, and differences in fragmentation patterns. There have been several attempts to demonstrate the utility of SID in fragmenting larger molecules. A collaborative study by Williams et al. first demonstrated the SID of peptides larger than 2000 Da in a dual-cell FTMS instrument.[34] The SID spectra of atriopeptin (MW = 2549), renin substrate (MW = 2281), and tetradecapeptide (MW = 3051) showed extensive fragmentation; however, the spectra depict mainly the low-mass portion of the spectrum (m/z 40−800). More recently, McLafferty and co-workers successfully fragmented carbonic anhydrase, a 29 000 Da molecule with SID in a cylindrical cell FTMS.[15] Their spectra yielded mainly low-abundance "b"- and "y"-type ions clustered around the precursor ion. Later, Wysocki et al. demonstrated a systematic SID study of multiply protonated peptides in a quadrupole mass spectrometer in the mass range of 2000−5000 Da [ACTH 18−39 (MW 2465), melittin (MW 2845), human β-endorphin (MW 3465), procine glucagon (MW 3484), oxidized bovine insulin chain-B (MW 3496), human parathyroid hormone 1−34 (MW 4118), and porcine ACTH 1−39 (MW 4568)].[9]

The Q-SID-TOF (quadrupole/SID/time-of-flight) design described here has been used to further extend the range of compounds amenable to SID. A broad range of molecules were explored, ranging from simple dipeptides (dialanine, diglycine) to larger peptides (such as YGGFL, YGGFLR, angiotensin, melittin, insulin chain-B), to larger protein complexes exceeding both the molecular weight and m/z range previously reported for SID (carbonic anhydrase (MW 29 000, m/z ~1261). The scope of this paper is focused mainly on SID of monomers of singly and multiply charged peptides and includes one example of dissociation of a large noncovalent complex. A discussion of dissociation of cytochrome *c* dimers by SID is presented elsewhere by Jones et al.[56] Discussion of the dissociation of a number of multimeric protein complexes will be published separately.[57]

A unique feature of the Q-SID-TOF instrument presented here is that it allows the direct comparison of CID and SID. This type of comparison, performed on the same instrument under the same experimental conditions and with the same samples, limits the possibility of experimental bias that may arise otherwise. For example, effects of mass-dependent ion transmission in the quadrupole, ion internal energy prior to collision, and kinetic energy distributions contributed by the source that may change with different instrumental source conditions are not a concern in this type of comparison.

SID of a Simple Peptide, YGGFL. To assess the performance of the Q-SID-TOF mass spectrometer and to enable comparison with previously published SID data, protonated leucine enkephalin (YGGFL) was selected as one reference molecule. Leucine enkephalin, a nonbasic pentapeptide has been fragmented in numerous studies, thus making it a useful molecule to test the performance of the new SID device. Figure 3 shows representative SID and CID spectra of YGGFL at collision energies of 30 and 35 eV, respectively (the CID and SID spectra shown here were selected in a way to match the appearances of the two spectra, not to match the collision energies). The experimental conditions for both SID and CID were kept identical (with the exception of the voltages used to focus ions in the SID device), to obtain an unbiased SID/CID comparison. The appearances of the two spectra are qualitatively similar and the resolution of the peaks in the Q-SID-TOF spectrum is approximately $m/\Delta m = 6000$ and is comparable to the resolution of the CID spectrum $m/\Delta m$ = ~6200 (it should be noted that the CID spectrum was acquired with the SID device installed).

Even though the two spectra are similar, there are some important differences. For example, a greater abundance of immonium ions such as those of leucine (m/z 86), phenylalanine (m/z 120), and tyrosine (m/z 136) are observed by SID (Figure 3a, top spectrum). These ions are high-energy secondary fragment ions[58] derived from further fragmentation of primary fragment ions or primary fragment ions formed by a rearrangement. The higher abundance of such ions in SID spectra suggests the translational (T) to internal (V) energy conversion is greater for SID. This is further supported by the intensity ratio of the doublet at m/z 278, 279 (b_3, y_2 ions of leucine enkephalin, respectively, Figure 3b). The intensity ratio of the b_3 fragment from leucine enkephalin to the y_2 fragment has been reported to be indicative of the extent of internal energy deposition.[59−61] The two left-hand panels of

(49) Beck, R. D.; Stjohn, P.; Homer, M. L.; Whetten, R. L. *Science* **1991**, *253*, 879−883.
(50) Yeretzian, C.; Beck, R. D.; Whetten, R. L. *Int. J. Mass Spectrom. Ion Processes* **1994**, *135*, 79−118.
(51) Williams, E. R.; Jones, G. C.; Fang, L.; Zare, R. N.; Garrison, B. J.; Brenner, D. W. *J. Am. Chem. Soc.* **1992**, *114*, 3207−3210.
(52) Williams, E. R.; Fang, L. L.; Zare, R. N. *Int. J. Mass Spectrom. Ion Processes* **1993**, *123*, 233−241.
(53) Gamage, C. M.; Fernandez, F. M.; Kuppannan, K.; Wysocki, V. H. *Anal. Chem.* **2004**, *76*, 5080−5091.
(54) Aberth, W. *Anal. Chem.* **1990**, *62*, 609−611.
(55) Schey, K. L.; Durkin, D. A.; Thornburg, K. R. *J. Am. Soc. Mass Spectrom.* **1995**, *6*, 257−263.
(56) Jones, C. M.; Beardsley, R. L.; Galhena, A. S.; Dagan, S.; Cheng, G. L.; Wysocki, V. H. *J. Am. Chem. Soc.* **2006**, *128*, 15044−15045.
(57) Beardsley, R. L.; Jones, C. M.; Galhena, A. S.; Wysocki, V. H. J. Manuscript in preperation.
(58) Laskin, J. *J. Phys. Chem.* A **2006**, *110*, 8554−8562.
(59) Alexander, A. J.; Boyd, R. K. *Int. J. Mass Spectrom.* **1989**, *90*, 211−240.
(60) Baeten, W.; Claereboudt, J.; Vandenheuvel, H.; Claeys, M. *Biomed. Environ Mass Spectrom.* **1989**, *18*, 727−732.
(61) Naylor, S.; Lamb, J. H. *Rapid Commun. Mass Spectrom.* **1990**, *4*, 251−255.

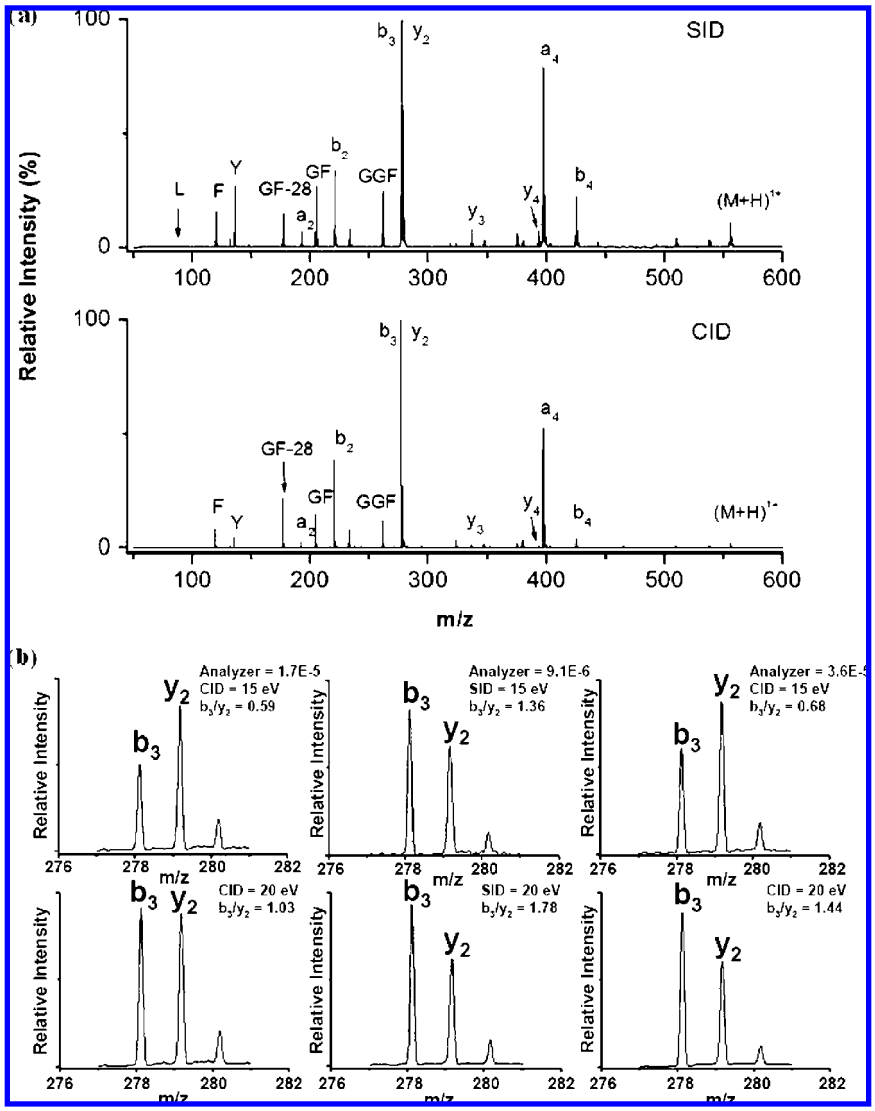

Figure 3. SID/CID comparison for singly charged leucine enkephalin (YGGFL). (a) SID at collision energy of 30 eV (top panel), CID at collision energy of 35 eV (bottom panel), and (b) relative b_3/y_2 intensities of CID and SID; left panel CID at quadrupole chamber pressure 1.7×10^{-5} mbar, middle panel SID, right panel CID at quadrupole chamber pressure 3.6×10^{-5} mbar.

Figure 3b show the b_3/y_2 ratio of leucine enkephalin observed by CID at low quadrupole chamber gas pressure (1.7×10^{-5} mbar) and demonstrate that, with increasing collision energy, more internal energy can be deposited (b_3/y_2 ratio changes from 0.59 to 1.03 as collision energy increased from 15 to 20 eV). Compared to low-pressure CID, SID indicates significantly higher internal energy deposition (by SID; the b_3/y_2 ratios are 1.36 and 1.78 at 15 and 20 eV, respectively, Figure 3b, middle) indicating SID provides greater internal energy deposition. Even at customary collision pressure (3.6×10^{-5} mbar), CID still deposits less internal energy than SID (Figure 3b, right), but to a lesser extent (ratio of b_3/y_2 changes from 0.68 to 1.44 at 15 and 20 eV collision energies). This can be explained by an increase in the number of collisions at higher argon pressure, which ultimately results in greater internal energy deposition. Comparing SID and CID (standard operational pressure 3×10^{-5} mbar) spectra of leucine enkephalin at similar collision energies shows that SID enhances the abundance of fragment ions, both in the low- and high-mass ends of the spectrum. This is attributed to the fact that SID is a high-energy activation process capable of depositing excess internal energy in a single step, allowing access to both the primary and secondary fragmentation processes within the time frame of the experiment (the b/a ratios of CID and SID also support this conclusion, where SID favors formation of high-energy secondary fragmentation a-ions at a given collision energy). With CID, these high-energy fragment ions can be observed at higher CID collision energies but only at the expense of the low-energy fragment ions in the high-mass region, consistent with stepwise activation by CID.

SID of Multiply and Singly Protonated Large Peptides. The utility of SID as an efficient tool to elucidate primary structures of peptides has been demonstrated previously. However, an important question still remains: can surface-induced dissociation be utilized to effectively fragment larger protonated compounds and thereby extend the analytical utility of this technique to fulfill the needs of the extending field of biological mass spectrometry? We have tested the new Q-SID-TOF instrument's capability to activate different peptides, proteins, and noncovalent protein complexes and present a few representative spectra (Figures 4−7) to illustrate its performance.

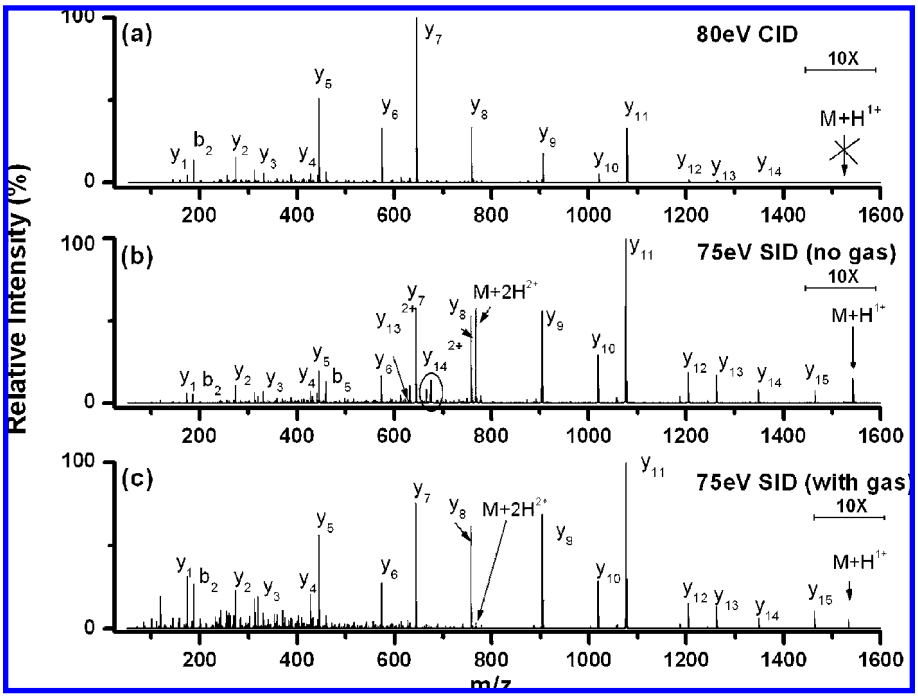

Figure 4. SID/CID comparison for doubly charged fibrinopeptide A. (a) CID at a collision energy of 80 eV ($\Delta V = 40$ V, corrected for 2+ charge state). (b) SID followed by CID in the gas-filled collision cell at 75 eV ($\Delta V = 37.5$ V), (c) SID at collision energy of 75 eV ($\Delta V = 37.5$ V).

As a general feature, with all of the large molecules we analyzed, the QTOF instrument was capable of generating high-quality spectra for both SID and CID. The total ion counts in fly-through mode were comparable to those obtained with the manufacturer's (CID only) QTOF setup. This result indicates, for the CID mode operation, that the SID device does not significantly attenuate ion transmission for a broad range of masses and energies, including the relatively slow higher mass projectiles and fragment ions. However, the SID mode of operation showed some sensitivity loss for larger molecules, but still it is capable of generating quality SID spectra. SID spectra of peptides yield mainly y-, b-, and a-type backbone cleavage ions, similar to CID. Although earlier studies reported that electronvolt SID could generate side-chain cleavages resulting in w- and v-type ions when generated from a high-energy liquid secondary ion mass spectrometry (LSIMS) ion source,[13] we have not observed significant abundance of side-chain cleavages in our ESI-QTOF- eV SID spectra. This is further supported by the studies done by Gu et al.,[62] where they proposed that the relatively high energies of precursor ions generated by an LSIMS source, compared to an ESI source, contributed to the formation of side-chain cleavage ions. While the differences in peptide fragmentation between the two ion activation methods are subtle, SID of simple ionic cluster systems such as $(CsI)_nCs^+$ differ significantly from their CID fragmentation patterns and will be published separately.

Another general feature of SID is charge reduction of multiply protonated peptides (as opposed to charge stripping of noncovalent complexes caused by removal of charged solvent adducts, which will be discussed later). As already reported,[9] precursor ions with charge state "n" can lose one charge upon SID to yield an "$n - 1$" charge species of the intact peptide. We observed the same behavior for SID (Figure 5) of multiply charged peptides, but not for CID. Charge reduction processes can be conceivably explained as a proton-transfer process from the projectile ion to the surface or electron transfer from the surface to the projectile ion. However, because the charge-reduced species in Q-SID-TOF correspond to loss of the mass of a proton, the charge reduction is the result of a loss of a proton, not addition of an electron. Recent studies by Laskin and co-workers, exploring soft landing on an FSAM surface, revealed the same behavior and it is believed that protons are readily transferred to FSAM surfaces.[63] The same phenomenon was observed by Tureček and co-workers for soft landing of peptides on plasma-treated stainless steel surfaces. Their experimental results also suggested that the mechanism of charge neutralization is a proton transfer from the peptide to the surface, a metal oxide in their experiment (followed by charge reduction of the protonated metal oxide by electron transfer from the conductance band of the buck metal).[64] Another plausible explanation for apparent charge reduction is the formation of multiply protonated multimers in the ion source (e.g., a triply charged trimer) that could overlap with monomer precursor ions during m/z selection by the quadrupole. Upon activation, these multimers could form monomers with lower charge states (further explained later). However, there is no direct experimental evidence to support this theory (isotope distribution of the precursor ion does not resemble a multiply charged multimer).

With CID, there is no observable charge reduction process. This can be explained by the fact that a noble gas atom such as argon is not a likely site to which H^+ transfer can occur and thus charge reduction does not occur. Furthermore, the gas-phase loss

(62) Gu, C. G.; Somogyi, A.; Wysocki, V. H.; Medzihradszky, K. F. *Anal. Chim. Acta* **1999**, *397*, 247−256.

(63) Alvarez, J.; Futrell, J. H.; Laskin, J. *J. Phys. Chem. A* **2006**, *110*, 1678−1687.

(64) Volny, M.; Elam, W. T.; Ratner, B. D.; Turecek, F. *Anal. Chem.* **2005**, *77*, 4846−4853.

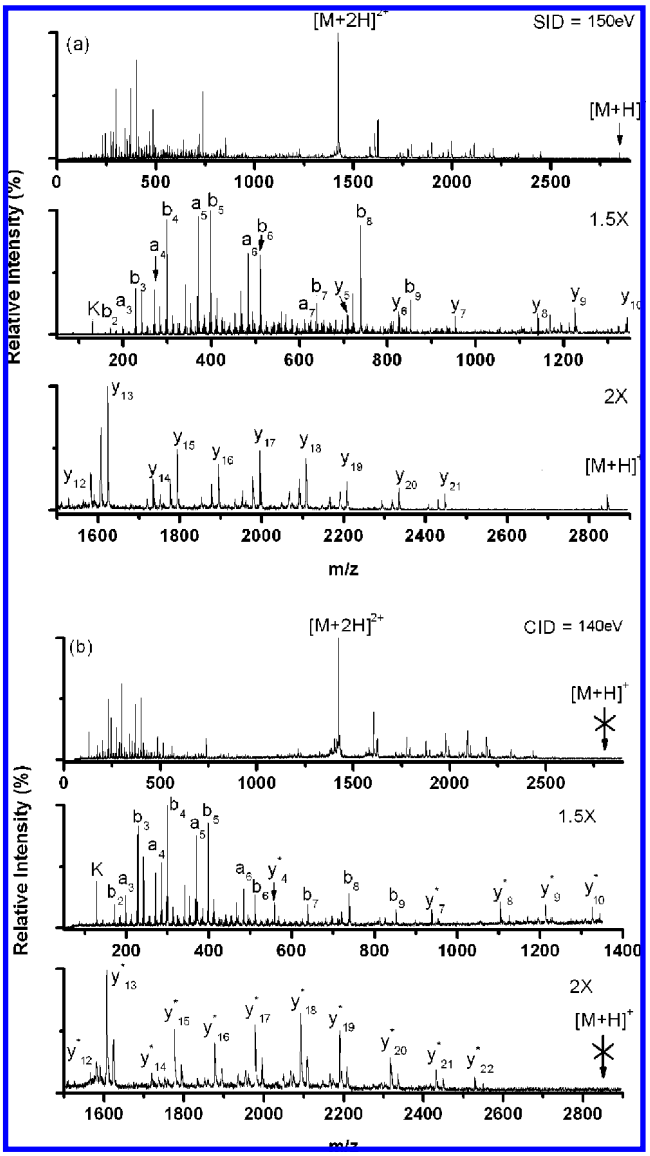

Figure 5. SID/CID comparison for doubly charged melittin. (a) SID at collision energy of 150 eV ($\Delta V = 75$ V) and (b) CID at collision energy of 140 eV $\Delta V = 70$ V). y* ions (CID) correspond to y − NH_3.

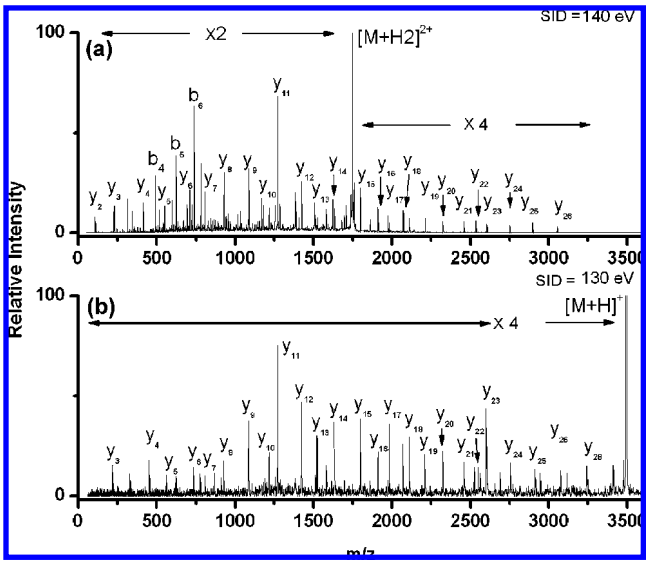

Figure 6. SID of bovine insulin chain-B. (a) SID of the doubly charged precursor ion at a collision energy of 140 eV ($\Delta V = 75$ V) and (b) SID of the singly charged precursor ion at a collision energy of 130 eV.

of a naked proton is also unlikely. The charge reduction behavior of SID can be useful in sequencing and can be employed to confirm the molecular mass and charge state of an unknown peptide.

Fibrinopeptide A. Doubly protonated fibrinopeptide A (m/z 768.78), a 16-residue peptide with the sequence of ADSGEGDFLAEGGGVR, was selected with the quadrupole mass analyzer and fragmented by CID, SID, or a combination of SID/CID. By either CID or SID (Figure 4a−c), an almost complete y-ion series was observed. In contrast the singly charged precursor ion generated a partially complete y-ion series (data not shown). This is expected as the doubly protonated peptide contains a greater number of protons (two) than the basic residues (one), thus providing a mobile proton to initiate cleavage along the peptide backbone and generate greater sequence coverage than fragmentation of the singly charged species. In Figure 4a, the 80 eV ($\Delta V = 40$ V, charge-state corrected) CID spectrum of doubly protonated fibrinopeptide A shows a complete conversion of the precursor ion to fragments. The SID spectrum, at 75 eV collision energy (Figure 4b), shows ∼50% precursor ion survival but still exhibits a very similar fragment ion distribution. Another interesting feature observed for SID of doubly protonated fibrinopeptide A was the charge reduction of the precursor ion (Figure 4b). As explained previously, the charge reduction behavior is confirmed as proton loss, not an electron addition.

By implementing an SID assembly that allows the original CID collision cell to remain unaltered in the instrument, SID products can be transmitted into a pressurized collision cell. Figure 4c shows an SID/CID combination spectrum in which the precursor ions were first collided into the surface, and the resulting product ions were transmitted into the gas-filled collision cell. At a lower argon pressure (∼20% of the typical CID pressure), there was no effect on the SID spectra (data not shown). However, the total ion count reading at the TOF detector (MCP) slightly increased at this elevated pressure, perhaps due to improved ion transmission. At the typical CID operating pressure suggested by the manufacturer (∼ 3.0×10^{-5} mbar in the quadrupole chamber region), the intensity of the precursor ion decreased while that of the fragment ions in the low m/z region increased. Although the intensities of some fragment ions were affected by the addition of gas, there were no additional product ions observed with the addition of gas (Figure 4b,c). The kinetic energy of the product ions after SID is much lower than that of the original incident precursor (experimentally measured as ∼3−10 eV); thus activation of these fragment ions by CID makes only a minor contribution. Furthermore, the doubly charged y-ions (Figure 4b, y_{14}^{2+}, y_{13}^{2+}) that appeared only in the SID spectrum became less abundant with the addition of the collision gas in the combination spectrum, suggesting that doubly charged fragment ions do not survive the CID activation.

Melittin. Melittin, a powerful anti-inflammatory substance found in bee venom, is another common peptide studied in previous CID and SID work. It contains 26 amino acid residues (GIGAVLKVLTTGLPALISWIKRKRQQ-NH_2) with an amide C-terminus. We have chosen this peptide because it contains

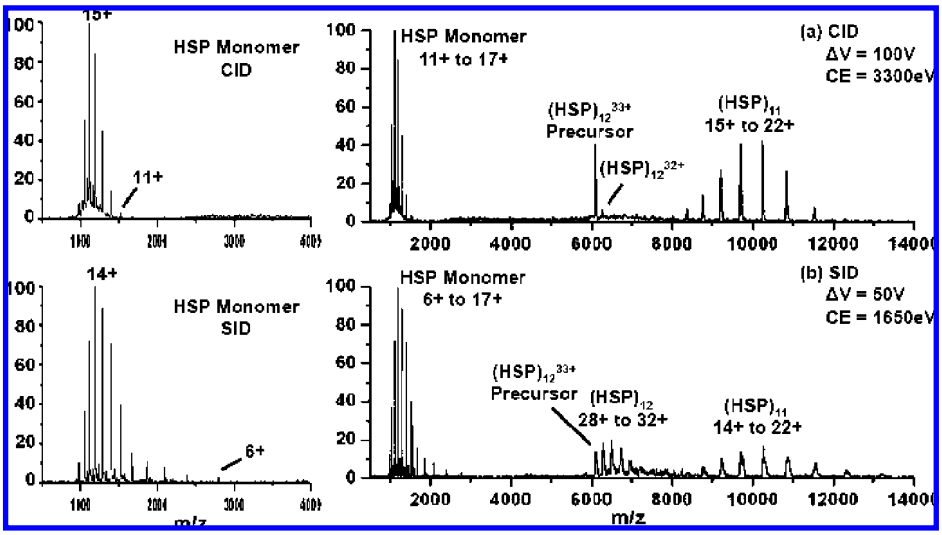

Figure 7. CID/SID comparison for the dodecameric protein complex *Ta*HSP16.9, 33+ charge state. (a) CID at $\Delta V = 100$ V, collision energy (CE) 3300 eV. On the left is an enhancement of the low *m*/*z* region containing monomer fragments centered about the 15+ charge state. (b) SID at $\Delta V = 50$ V, CE = 1650 eV. The left-hand side is the enhancement of the monomer region centered about the 14+ charge state.

multiple basic residues. This allows us to choose a charge state for fragmentation in which the number of basic residues exceeds the number of protons, in a peptide with no acidic residues, making fragmentation more difficult.

Figure 5a shows the SID spectrum of doubly protonated melittin (m/z 1424.25), which yields a dominant singly charged y-ion series at a collision energy of 150 eV ($\Delta V = 75$ V). The generation of a complete y-ion series can be explained by the presence of basic residues (KRKR) close to the C-terminus, whereas only a partial series of b-ions is observed. Unlike the SID spectra reported by McLafferty et al.[15] (for the quadruply protonated precursor) and Wysocki et al.[8] (for the doubly protonated precursor) in FTICR and quadrupole-surface-quadrupole instruments, respectively, QTOF SID spectra of doubly protonated melittin were not lacking any of the y-ions in the series, from y_2 to y_{21} (although the intensity of y-ions from y_2 to y_5 is low). In addition to y-ions, another series of satellite peaks corresponding to formal losses of 17 (NH_3)and 45 Da ($NH_3 + CO$) from the y-ions were observed for both the SID and CID spectra and can be explained by the presence of a C-terminal amide group. One of the major differences between SID and CID spectra is that SID showed a dominant y-ion series (Figure 5a), whereas CID (Figure 5b) showed a dominant [y − NH_3] series (y*). A possible reason for the above difference is the multiple collision nature of CID, which may facilitate the secondary [y − NH_3] fragmentation pathways. Another difference observed for the two spectra is the slightly enhanced b-ion series of SID, especially b_8. In addition, charge reduction is also observed by SID whereas none of the CID spectra show any charge reduction behavior.

Bovine Insulin Chain-B (Oxidized). Bovine insulin chain-B (oxidized), a 30-residue peptide with the sequence FVNQHLuGSHLVEALYLVuGERGFFYTPKA (*u* = cysteic acid), was analyzed by selecting the doubly and the singly protonated precursor ions (m/z 1749.9 and 3496.9, respectively) in two different SID experiments. Insulin chain-B generates a combination of y- and b-type backbone cleavage ions for both the doubly and singly charged species. The fragmentation efficiencies for both the charge states are shown to be relatively low, similar to that of 2+ melittin. This is attributed to the fact that the two protons of doubly protonated insulin chain-B are localized at the most basic sites of the peptide, lysine and arginine (for the singly charged peptide, it is expected to be localized at arginine). Hence, excess energy is needed to mobilize the protons prior to fragmentation and the backbone fragmentation is less favorable. Once a sufficient amount of energy is added, however, extensive sequence coverage is achieved. Figure 6a shows the SID spectrum of doubly protonated insulin chain-B at a collision energy of 140 eV ($\Delta V = 70$ V). A contiguous singly charged y-ion series covering the sequence from y_2 to y_{26} and a contiguous singly charged b-ion series covering the sequence from b_2 to b_{18} (not labeled) is observed with doubly charged insulin chain-B. Generation of an almost complete y-ion series can be predicted due to the presence of lysine and arginine near the C-terminus. This phenomenon is a well-established concept and is consistent with the position of the basic residue in the peptide/protein chain influencing the type of ions observed in the spectra due to sequestering of the protons at the most basic sites.[65] Another prominent feature of the spectrum is the appearance of enhanced y_{11} fragment ion corresponding to a C-terminal cleavage of cysteic acid. This phenomenon is also expected. Gaskell and co-workers have reported significant enhancement of the fragmentation C-terminal to cysteic acid.[66,67]

For SID of insulin chain-B, as with other large peptides, the peaks appearing above the mass/charge of the precursor ion (m/z 1748.9) were less intense in comparison to peaks below the mass/charge of the precursor ion. A plausible reason for such low abundance could be attributed to the difficulty of focusing the high mass-to-charge ions with the SID device (see below for further explanation).

Figure 6b shows the SID spectrum of singly protonated insulin B at a collision energy of 130 eV ($\Delta V = 130$ V). Compared to SID of doubly protonated insulin chain-B, singly charged insulin

(65) Tabb, D. L.; Huang, Y. Y.; Wysocki, V. H.; Yates, J. R. *Anal. Chem.* **2004**, *76*, 1243−1248.
(66) Summerfield, S. G.; Whiting, A.; Gaskell, S. J. *Int. J. Mass Spectrom. Ion Processes* **1997**, *162*, 149−161.
(67) Cox, K. A.; Gaskell, S. J.; Morris, M.; Whiting, A. *J. Am. Soc. Mass Spectrom.* **1996**, *7*, 759−759.

chain-B shows a slightly higher survival of the molecular ion. Furthermore, the sensitivity (total ion count at the MCP detector) is shown to be lower by a factor of ~2−3 for the singly charged insulin chain-B compared to the doubly charged species. One of the reasons for this decrease in sensitivity is the lower abundance of the singly charged species in the MS spectrum of insulin chain-B. Another possible reason for the sensitivity loss is the reduced ion focusing capability of the SID device for slow moving larger ions. A fundamental problem with transmitting high-mass projectiles with fewer charges (in this case insulin B chain with one charge) is the influence of the electric field with respect to the mass of the projectile ion (this is true for noncovalent complexes discussed in the following section). Since these ions have a high mass-to-charge ratio, focusing is more challenging, as those slow-moving ions are likely to suffer from radial dispersion (note: Both the low- and high-mass ions have radially distributed kinetic energies. However, the acceleration of low m/z ions in the axial direction is more effective than that of high m/z ions and any radial kinetic energy dispersions of low m/z ions are compensated to some extent.). Our latest generation of SID device proved to be the most effective in transmitting ions over a broad range of m/z values. Thus, even though the SID spectrum is slightly less sensitive for singly protonated insulin chain-B, considering the high quality of the SID spectrum, the sensitivity drop does not significantly hinder the performance of the device. The SID spectrum of MH^+ (Figure 6b) clearly shows a prominent y-ion series from y_3 to y_{28}. Once again enhanced fragmentation C-terminal to the cysteic acid is evidenced by the abundant y_{11} and y_{23} fragments.

Noncovalent Protein Complexes. To evaluate the CID/SID performance for noncovalent complexes in the Q-SID-TOF instrument, a heat shock protein (HSP) from wheat, *Ta*HSP16.9, was chosen, as it has been previously characterized by mass spectrometry.[68,69] At room temperature, *Ta*HSP16.9 exists as a dodecamer, having 12 identical subunits each with a molecular mass of 16.9 kDa, and an overall molecular mass of ~201 kDa for the intact complex.

The motivation for studying a noncovalent protein complex was 2-fold. First, it allowed the efficiency of SID to be examined for large molecules. As ion size increases, the efficiency of fragmentation in MS/MS experiments is hindered by a decrease in the center-of-mass collision energy and an increase in the number of internal modes into which energy can be redistributed. To our knowledge, *Ta*HSP16.9, and the closely related *Ps*HSP18.1 (pea) dodecamer,[70] are the largest systems explored by SID to date, and the efficiency of internal energy transfer relative to CID for ions in this mass regime was of interest.

Second, CID of most noncovalent complexes has been characterized by an asymmetric partitioning of both mass and charge. We have previously observed that SID of small dimeric and tetrameric protein complexes demonstrates relatively more symmetric partitioning of both mass and charge than those produced via CID.[56,57] We were interested in exploring whether or not CID and SID differ for even larger complexes.

Figure 7a shows the CID spectrum of the 33+ *Ta*HSP16.9 dodecamer. The precursor ion was selected with the quadrupole mass analyzer and accelerated into the argon-filled collision cell (gas pressure 1×10^{-4} mbar at the quadrupole chamber Penning gauge). The acceleration voltage was set to 100 V, corresponding to a collision energy of 3330 eV after correcting for charge state.

The major CID product ions are monomers ranging in charge state from 11+ to 17+, with the distribution centered about the 15+ monomer at m/z 1115 (see enhanced monomer region on the left of Figure 7a). These monomers retain approximately half the charge of the precursor ion, an asymmetric dissociation of the original dodecamer in terms of both mass and charge. Complementary undecameric subunits are observed at the high m/z end of the spectrum, centered about the 18+ charge state. In addition to monomer and undecamer fragments, 32+ dodecameric ions are also observed. This can be attributed to the loss of ammonium buffer ions from the dodecameric complex, resulting in ions that have "lost" charge relative to the original precursor.[71]

SID of the 33+ dodecamer is shown in Figure 7b. The predominant fragment ions observed are undecamers and monomers, as in the case of CID. There are, however, some striking differences between the two spectra. In the SID spectrum, as many as six charge states of the dodecameric protein are observed (from the original 33+ down to the 28+ charge state). At this point, it is unclear whether the presence of these lower charge states is due solely to a greater sequential loss of ammonium ions.

The other distinction between the CID and SID spectra is the distribution of the monomeric charge states. SID of the 33+ precursor yields a monomer distribution centered about the 14+ charge state, shifted slightly from the 15+ charge state in the CID spectrum. In the SID spectrum, however, monomers ranging in charge state from 17+ all the way out to 6+ at m/z 2787 are observed (vs 17+ to 11+ for CID). The charge retained by the ejected monomer has been correlated to the monomer's surface area as it unfolds and dissociates from the remaining complex.[72] Thus, a lower charge-state distribution could indicate that the monomer ejected during SID is in a more compact or folded conformation than that ejected by CID. The possibility that the lower charge states in the SID spectrum result from the dissociation of a charge-stripped dodecamer, however, cannot be ruled out. For example, the 33+ dodecamer might first undergo loss of solvent to yield a lower charge state (i.e., the 30+ dodecamer, which is not observed by CID), followed by ejection of a monomer. If the dodecameric complex loses charge prior to dissociation, the ejected monomer would be expected to retain fewer charges, even if the conformation of the monomer were similar to that ejected during CID. The charge states observed for the undecamer fragments are similar in both cases.

The relative collision energy required to induce fragmentation by SID is also of interest. While the two spectra in Figure 7 show similar levels of precursor ion depletion, the laboratory collision energy in the SID spectrum is exactly half of the laboratory collision energy applied to produce the CID spectrum. The onset

(68) Sobott, F.; Benesch, J. L. P.; Vierling, E.; Robinson, C. V. *J. Biol. Chem.* **2002**, *277*, 38921−38929.

(69) Benesch, J. L. P.; Sobott, F.; Robinson, C. V. *Anal. Chem.* **2003**, *75*, 2208−2214.

(70) Wysocki, V. H. J., K. E.; Jones, C. M.; Beardsley, R. L. *J. Am. Soc. Mass Spectrom.* Submitted.

(71) Sobott, F.; McCammon, M. G.; Robinson, C. V. *Int. J. Mass Spectrom.* **2003**, *230*, 193−200.

(72) Benesch, J. L. P.; Aquilina, J. A.; Ruotolo, B. T.; Sobott, F.; Robinson, C. V. *Chem. Biol.* **2006**, *13*, 597−605.

(73) van Duijn, E.; Simmons, D. A.; van den Heuvel, R. H. H.; Bakkes, P. J.; van Heerikhuizen, H.; Heeren, R. M. A.; Robinson, C. V.; van der Vies, S. M.; Heck, A. J. R. *J. Am. Chem. Soc.* **2006**, *128*, 4694−4702.

of dissociation in these two cases occurs at ~2640 eV for CID, but only ~1320 eV for SID (data not shown). This shows promise for the use of SID in the dissociation of complexes that have proven too large and stable to fragment by CID.[73]

CONCLUSIONS

A novel in-line SID device, which allows direct comparison of CID and SID on the same instrument, has been designed and implemented in a quadrupole/time-of-flight mass spectrometer. The operation of the SID device is robust and efficient. It allows for high-quality SID tandem mass spectra of high m/z precursor ions, including large peptides and noncovalent protein complexes.

The SID product ion spectra of peptides were highly resolved, informative and in general similar to CID, with some observed differences in relative abundances of particular fragments. The SID of protonated peptides predominantly generated backbone cleavage a-, b-, y-type, and immonium ions. Compared to CID, SID revealed higher ratios of a- to b-ions, and enhanced immonium ions. This is an indication of increased accessibility to high-energy/secondary fragmentation channels with SID. SID also showed a distinct feature of charge reduction for multiply charged projectiles. This may be a complementary tool for identification of multiply charged projectiles. The SID of noncovalent complexes also revealed some differences compared to CID. First, dissociation of noncovalent complexes by SID can be achieved at nearly half the laboratory collision energy required for dissociation by CID. Second, there is a greater number of charge-stripped products by SID, and finally, a broader monomer charge state distribution is observed by SID.

The new and effective Q-SID-TOF setup proved to be a feasible alternative to conventional CID for peptides and complexes of proteins with several potential advantages over CID (no collision gas, and energy deposition in a single, fast step). In the future, the novel Q-SID/CID-TOF configuration may allow more detailed explorations of the energy deposition/distribution channels of SID in relation to CID. Furthermore, this type of instrument provides a unique platform for future research involving the study of the dissociation of very large complexes by different activation methods or combination of those methods.

ACKNOWLEDGMENT

This material is based upon work supported by the National Science Foundation under Grant DBI-0244437. The authors thank Professor Elizabeth Verling for providing sHSP samples. We thank Facundo Fernandez for helpful discussions. We also gratefully acknowledge the support provided by Micromass/Waters Corporation.

Received for review August 22, 2007. Accepted October 19, 2007.

AC701782Q